
Assessing Intratumor Distribution and Uptake with MBBG Versus MIBG Imaging and Targeting Xenografted PC12-Pheochromocytoma Cell Line

Jérôme Clerc, Karine Mardon, Hervé Galons, Christian Loc'h, Jean Lumbroso, Pascal Merlet, Jiarong Zhu, Josette Jeusset, André Syrota and Philippe Fragu

Equipe de Microscopie Ionique, INSERM, Institut Gustave Roussy, Villejuif, France; Laboratoire de Chimie Organique 2, Université René Descartes-Paris V, Paris, France; Service Hospitalier Frédéric Joliot, DRIPP-CEA, Orsay, France; and Service de Médecine Nucléaire, Institut Gustave Roussy, Villejuif, France

The heterogeneity of tumor uptake is likely to substantially limit the effectiveness of metaiodobenzylguanidine (MIBG) therapy. This study was done to establish whether metabromobenzylguanidine (MBBG) can target neuroendocrine tumors and to provide intratumor biodistribution and uptake information in comparison to MIBG. **Methods:** MBBG and MIBG tumor uptake and kinetic studies were performed in experimental PC-12 pheochromocytoma grown in nude mice. Intratumor distribution studies were performed using autoradiography and secondary ion mass spectrometry (SIMS) microscopy, because the latter technique can detect and potentially quantify both drugs concomitantly within the same tumor specimen. **Results:** MBBG uptake in PC-12 tumors was early (2 hr) and intense (80% ID/g). Retention values were similar for both drugs 24 hr postinjection. At the cellular level, MBBG mostly accumulated in the cytosol. At the multicellular level, cells exhibited staining, but in many areas, SIMS images of both drugs were not spatially correlated. **Conclusion:** MBBG targeted experimental pheochromocytoma efficiently with high early uptake values. Bromine-76-MBBG is a promising means of imaging and quantifying tumor uptake with PET. Both drugs were localized in the cytosol, but the correlation between the two distributions, as assessed by the values of the standardized local concentrations, was weak although significant multicellularity.

Key Words: secondary ion mass spectroscopy microscopy; metabromobenzylguanidine; metaiodobenzylguanidine; pheochromocytoma; metabolic radiotherapy

J Nucl Med 1995; 36:859–866

After more than a decade of worldwide experience with metabolic radiotherapy of neural crest tumors using labeled metaiodobenzylguanidine (MIBG), many areas of

uncertainty and deficiency remain to be explored (1). Problems encountered in radiation dosimetry remain a challenge (2). Preradiation therapy dosimetry methods have been developing intensively since 1991 so that the absorbed dose received by the bone marrow, the dose-limiting organ, can be more accurately predicted (3). No clear-cut relationship had been reported, however, between response and the whole-body radiation dose, which is itself contingent on the total activity administered.

Only mean tumor absorbed doses of 10 Gy or more would provide both significant and prolonged clinical effects (4). Tumor dosimetry, however, is still rather rudimentary because of the difficulty to determine targeted functioning volumes accurately with conventional imaging techniques (CT or MRI), especially when there is bone marrow involvement (2,5). In addition, external detection and quantification of tumor radioactivity may be distorted by background activity. Therefore the use of the conjugate view technique and, more recently, pretherapy administration of the positron-emitting tracer [¹²⁴I]MIBG-labeled variant to predict the actual [¹³¹I]MIBG mean absorbed dose appears promising (6,7).

The tumoricidal effects of radiolabeled MIBG are contingent on two main factors: (1) the tumor's capacity to take up and retain the tracer and (2) its intratumoral pattern of biodistribution. Attempts have already been made to improve the first factor; gamma-interferon and retinoic acid have been shown to increase MIBG accumulation in vitro, although no clinical trials investigating such pharmacological intervention have been reported (8,9). With respect to the second factor, it is necessary to determine the best isotope to attach to MIBG, or alternative halogenated analogs, taking into account tracer biodistribution in the target, so that every tumor cell will be effectively irradiated. Bromine-76-metabromobenzylguanidine (MBBG) was recently proposed to explore sympathetic innervation in the heart (10). This ⁷⁶Br-labeled MIBG analog appears to possess adequate parameters for imaging and metabolic

Received Jul. 6, 1994; revision accepted Nov. 23, 1994.
For correspondence or reprints contact: Dr Jérôme Clerc, Department of Nuclear Medicine A, Necker Hospital, 149 rue de Sèvres, 75743 Paris Cedex 15, France.

radiotherapy and its ability to target bioamine receptor-positive tumors was evaluated. Both drugs were administered to nude mice xenografted with the PC12 rat pheochromocytoma, a cell line known to actively store MIBG *in vitro*. In addition, as data on tracer biodistribution are needed for microdosimetric evaluation, we capitalized upon a unique possibility offered by secondary ion mass spectrometry (SIMS), namely intratumor mapping and quantification of MBBG using MIBG as the reference tracer. SIMS microscopy is a microanalytical technique based on two principles in physics: the emission of secondary ions following the bombardment of a specimen by a primary ion beam and mass spectrometry (11). With SIMS, it is theoretically possible to visualize biodistribution of any stable or radioactive ion species within biological material and quantify the signal using an internal standard. Based on our findings with the PC12 experimental pheochromocytoma xenografted into mice, MBBG appears to be a promising tracer for the work-up of neural-crest tumors.

MATERIAL AND METHODS

Cells and Experimental Tumors

The rat pheochromocytoma cell line PC12 was shown to store dopamine, norepinephrine and more recently MIBG (12). This drug is first taken up at the membrane level through the neuron-specific uptake-1 mechanism, which is energy-dependent and saturates at 10^{-6} M. Once in the cell, MIBG is stored in specialized granules, particularly numerous in pheochromocytoma, through a so called uptake-3 system (4). This system requires a proton pump and is inhibited by reserpine. The cells were propagated in a RPMI 1640 medium containing 15% horse serum and 5% fetal calf serum plus antibiotics. Several series of 6–8-wk-old pre-irradiated (5 Gy) nude mice (SP Swiss nu/nu mice, 10 mice per series) were injected subcutaneously in the flanks with approximately 3×10^7 cells. Small tumors (50–200 mg) were obtained about 3 wk later.

Radlpharmaceuticals

The synthesis and pharmacological preparation of [^{76}Br]MBBG has been reported elsewhere (13). Briefly, ammonium (^{76}Br) bromide is produced by the irradiation of natural arsenic with a 30-MeV (^3He) ion beam. Then, [^{76}Br]MBBG is prepared by heteroisotopic exchange between the [^{76}Br]BrNH₄ and the cold iodine atoms of MIBG using a Cu⁺ assisted substitution reaction. Bromine-76-MBBG is separated from the iodo precursor by HPLC and finally dissolved in saline and filtered onto a 0.22- μm Millipore membrane. The radiopharmaceutical is produced in a 65% radiochemical yield with a specific activity of 20 MBq/nmole.

The synthesis of stable MBBG was required for SIMS experiments because the weight of the injected amounts of the radioactive brominated analog was clearly below the detection sensitivity of the SIMS microscope. The synthesis of MBBG sulfate was achieved after condensation of 3-bromobenzylamine hydrochloride (3.34 g, 15 mmole) with 2-methyl-2-thiopseudourea sulfate (5.16 g, 30 mmole) in the presence of dimethylformamide (DMF), which was found to facilitate the reaction. Briefly, a mixture of the two precursors in 20 ml DMF was heated at 100°C for 4 hr. After cooling, the solvent was distilled under vacuo. The resulting solid was dissolved in 150 ml of isopropanol and left overnight at 4°C. The white crystals were isolated by filtration and recrystallized

from isopropanol: 2.25, yield: 48%. Specific spectra of the final molecule were obtained: IR(KBr): 2200–3300 cm^{-1} , 1640 cm^{-1} ; ¹H-NMR (DMSO-d₆, TMS) δ : 3.95 (s, 2H), 7.31 (m, 2H), 7.51 (dd, 1H), 8–9.2 (s, large, 5H). The crystal was weighed, resuspended in saline and sterilized as above.

The MIBG, [^{127}I]MIBG (1300 $\mu\text{g}/400 \mu\text{l}$), used in the SIMS experiments was kindly provided by CIS-Bio International (Gif-sur-Yvette, France), as well as [^{125}I]MIBG (~0.4 MBq/nmole) for autoradiographic purposes. Iodine-123-MIBG was used for gamma camera imaging and counting purposes at a specific activity of about 0.05 MBq/nmole.

Protocols

Bromine-76-MBBG uptake by the tumors and various organs was determined 2, 4, 8, 12, 19 and 24 hr after injection of about 74 kBq in the tail vein. Parallel uptake experiments were performed with [^{123}I]MIBG 8 and 24 hr after intraperitoneal injection of about 1100–1850 kBq. In all cases, the samples were weighed, radioactivity was measured in a gamma well-counter and results were expressed as a percentage of the injected dose per gram (%ID/g).

Macroscopic Imaging

Whole Mouse Body Autoradiography with [^{76}Br]MBBG. Ethyl-ether anesthetized animals who had received 1110 kBq [^{76}Br]MBBG were frozen, 8 hr postinjection in an ice-isopentane solution (–75°C) and then placed into a cold solution of carboxymethylcellulose (CMC-1.5%) to permit rough sectioning (20 μm) in a cryomicrotome. Precooled adhesive tape was applied on the tissue slice to remove sections that were further dried and exposed for 10 days on autoradiographic films. Films were developed, analyzed and color-coded using a computerized densitometric system.

Nuclear Imaging. Five mice injected with [^{123}I]MIBG underwent scintigraphic studies 10, 19 and 24 hr postinjection. Each animal was anesthetized three times with ketamine (15 $\mu\text{g}/\text{g}$) and images were acquired on a DSX gamma camera (Sopha Médical, Buc, France) equipped with a high-resolution, parallel-hole collimator. An aliquot (370 kBq) of the administered tracer was also imaged as an internal standard and tumor uptake was determined with ROI method with background correction for extratumor activity estimated on the tumor-free flank. Finally, 24-hr MIBG scintigraphic uptake in tumors was compared to the values obtained through direct gamma well counting as described above. Two additional mice bearing the nontargeted neuroblastoma IGR-N-835 were used as controls (14).

Microscopic Imaging

MIBG Microautoradiography. Two animals received about 1850 kBq of [^{125}I]MIBG and were killed 24 hr later. Chemical sample processing (see below) was performed and 2- μm sections of the specimen were mounted on slides, coated with Amersham LM1 emulsion, exposed for 8–20 days and finally stained with hematoxylin-eosin.

SIMS Analysis. Stable MBBG was injected into the animals intraperitoneally by escalating dose increments (0, 100, 200, 400, 600 μg). In addition, 400 μg of [^{127}I]MIBG were concomitantly injected into mice, who received 200–400 μg of MBBG. All animals were killed 24 hr later.

Fixative Procedures, Embedding and Sectioning. Sample processing was performed using either a chemical or a cryo-procedure as previously described. With the chemical procedure, which cannot prevent drug diffusion, fragments are fixed in glutaraldehyde and paraformaldehyde in cacodylate buffer and finally resin-

TABLE 1
Biodistribution (%ID/g) of [⁷⁶Br]MBBG and [¹²³I]MIBG in Nude Mice Xenografted with the PC12 Pheochromocytoma Cell Line*

Tissues	4 hr	8 hr	12 hr	24 hr
Tumor	32.6 ± 3.3	82.3 ± 7.2 <i>21.6 ± 4.0^f</i>	53.3 ± 4.9	20.2 ± 3.7 <i>19.4 ± 5.4</i>
Heart	4.34 ± 0.67	5.12 ± 0.55 <i>1.8 ± 0.2^f</i>	2.30 ± 0.66	0.93 ± 0.32 <i>0.45 ± 0.15^f</i>
Lungs	2.95 ± 0.30	2.93 ± 0.54 <i>1.5 ± 0.24^f</i>	1.72 ± 0.30	0.87 ± 0.15 <i>0.47 ± 0.05^f</i>
Liver	2.73 ± 0.37	2.11 ± 0.24 <i>1.36 ± 0.18^f</i>	1.33 ± 0.34	0.54 ± 0.10 <i>0.48 ± 0.02</i>
Spleen	1.54 ± 0.48	3.19 ± 0.67 <i>1.45 ± 0.30^f</i>	2.31 ± 0.96	0.79 ± 0.38 <i>0.66 ± 0.14</i>
Adrenals	6.20 ± 0.55	18.7 ± 4.3 <i>5.09 ± 0.93^f</i>	12.9 ± 2.5	6.5 ± 1.5 <i>3.9 ± 1.6^f</i>
Muscle	0.51 ± 0.05	0.75 ± 0.11 <i>0.32 ± 0.09^f</i>	0.76 ± 0.19	0.3 ± 0.07 <i>0.18 ± 0.03^f</i>

*Values are presented in boldface for MBBG and in italics for MIBG.

^fp < 0.05. MBBG and MIBG uptake values were compared using the Bonferroni's t-test with a risk of 0.05. Uptake kinetic studies were performed at all times for MBBG (bold characters) but only at 8 and 24 hr postinjection for [¹²³I]MIBG. All mice had PC12 xenografts obtained directly from tumor cells. Activities used for these experiments were typically in the range of 75 kBq of [⁷⁶Br]MBBG (specific activity: 20 MBq/nmole) and 750 kBq of [¹²³I]MIBG (specific activity: 0.05 MBq/nmole). Differences in early uptake values may reflect differences in the routes of administration, intraperitoneally for MIBG and intravenously for MBBG.

embedded. The cryomethods, which allow in situ immobilization of diffusible drugs, consist in high-speed freezing (5000 Ksec⁻¹) in liquid propan, cryo-substitution in acetone (183K) and cryo-embedding (213K) in Lowicryl K11M (Polysciences Ltd., Eppenheim, Germany). Semi-thin sections (3 μm) were deposited on ultrapure gold holders for SIMS analysis.

SIMS Microscopy Imaging. Description of the IMS-3F microscope (Cameca, Courbevoie, France) has been reported elsewhere (15). Briefly, a 5–15-nA primary cesium ion beam is focused on the surface of the resin-embedded specimen to sputter and possibly ionize the atoms located in the superficial layers (1–5 nm). The secondary ions, characteristic of the atomic composition of the analyzed area, are focused, energy-filtered and separated in a mass spectrometer. The ion images are finally displayed using a highly sensitive camera and a dedicated microcomputer system (16). All images are acquired with high mass resolution (M/ΔM > 2000) to guarantee signal specificity because cluster ions are emitted close (<0.07 uma) to the ions of interest (17). SIMS analysis progressively erodes the specimen at a destruction rate of about 1.5 nm/sec and provides images with a 500-nm resolution for a detection sensitivity of less than 1 ppm for halogens. The tissue structure can be visualized through the mapping of the polyatomic ion ²⁶CN⁻, the nuclei of the cells through ³¹P⁻, whereas drug biodistribution is delineated through detection of ¹²⁷I⁻ (MIBG) and ⁷⁹Br⁻ or ⁸¹Br⁻ (MBBG) because bromine has two stable isotopes of similar abundance: ⁷⁹Br⁻ (50.57%) and ⁸¹Br⁻ (49.43%).

Quantification with SIMS Microscopy. The secondary ion beam intensity can be measured with an electron multiplier and is proportional to the corresponding elemental concentration and to the primary ion beam intensity. The primary beam, however, is partly repelled by charge effects occurring at the surface of the embedded insulating specimen. Because carbon is present at a large and rather homogeneous concentration in the specimen, as well as in the resins, it can be used as an internal reference. Tissue equivalent resin standards containing increasing proportions of

halogens had been synthesized to derive calibration curves between isotopic ratios (ion of interest/carbon reference) and concentrations (18). We used 8 μm wide apertures, which can be superimposed onto an ²⁶CN⁻ ion image (62 μm) and cycles of 10 consecutive 1-sec measurements were acquired. Counting was performed on cryoprepared fragments for the 200- and 400-μg injected dose levels.

RESULTS

Bromine-76 MBBG Uptake in PC12 Xenografted Mice

Tumor and tissue concentrations of both radiopharmaceuticals are given in Table 1. Tumor tissue had the highest and most prolonged uptake. MBBG strongly accumulated in tumors, even early after administration (2–4 hr), with a peak value as high as 80% ID/g at 8 hr postinjection, but a significant reduction in uptake occurred between 8 and 24 hr. Comparisons between the targeting efficacies of MBBG and MIBG must be interpreted with caution in these experiments since molar drug doses and specific activities used were very different for both drugs. In addition, lower early uptake values encountered with MIBG (intraperitoneally) as compared to MBBG (intravenously) may partly reflect the routes of administration.

Macroautoradiography and Gamma Camera Images

The whole-body autoradiogram (Fig. 1) displays [⁷⁶Br]-MBBG accumulation at the periphery of the tumor. There was partial central necrosis, which may be overlooked on planar scintigraphic images. Gamma camera images of a panel of 3 PC-12 mice showed intense accumulation of [¹²³I]MIBG, at any time postinjection (Fig. 2). Tumor uptake, as determined from the scans and using the actual weight of the tumor obtained after dissection, was 25.1 ± 4.1, 24.2 ± 6.6 and 17.5 ± 6.5% ID/g 10, 17 and 24 hr

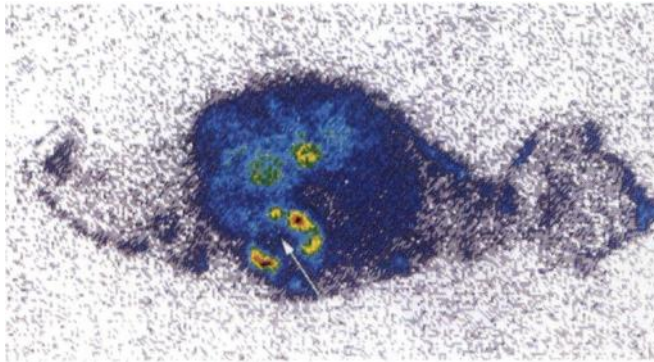


FIGURE 1. Whole-body autoradiogram of a mouse bearing the PC12 pheochromocytoma xenograft injected with [^{78}Br]MBBG (1110 kBq) 8 hr before death. The analyzed image, facilitated by a display using pseudocolors, shows strong accumulation of MBBG only at the periphery of the tumor because its center is necrotic (arrow).

postinjection, respectively. If one excludes one mouse, for which tumor dissection had been incomplete, uptake values derived from scanning and tumor counting correlated closely ($r = 0.96$, $p < 0.05$, $n = 6$).

Iodine-125 MIBG Imaging of Tumors by Microautoradiography

Due to the strong affinity of tumors for MIBG, intense staining was observed after 12 days of exposure (Fig. 3). Most of the cells had accumulated MIBG and exhibited a rather homogeneous pattern of distribution at the tissue level. At the cellular level, staining mainly affected the cytosol. Some silver grains were also evidenced, however, on cell nuclei because the chemical sample processing method used here cannot prevent MIBG diffusion from

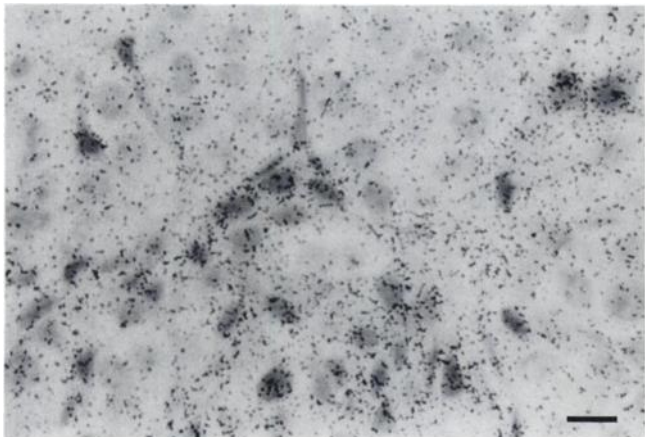


FIGURE 3. Autoradiography of PC12 pheochromocytoma xenografted into mice injected intraperitoneally with 1850 kBq of [^{125}I]MIBG and killed 24 hr later. Samples were exposed for 12 days and colored with hematoxylin-eosin. According to the tumor model, most of the cells are stained, particularly those close to the lumen of vessels. At the cellular level, however, the silver grains are evidenced both in the cytosol and in the nuclei because the chemical sample processing method was inadequate (Bar = 5 μm).

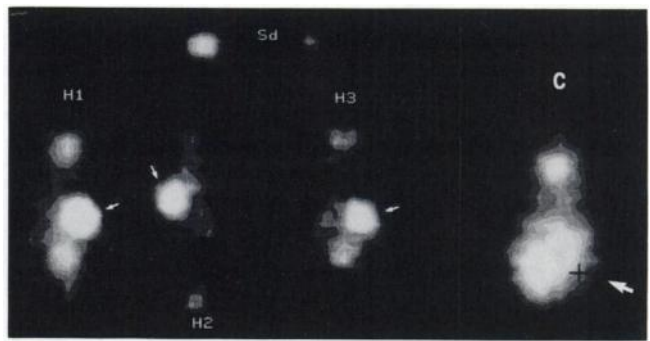


FIGURE 2. Gamma camera images of a panel of three PC12-xenografted nude mice injected with [^{123}I]MIBG (1110 kBq administered intraperitoneally). The image (50 kcts, posterior view) was acquired 10 hr postinjection. There is intense tracer accumulation in the xenografts, readily visible in the flanks (small arrows). No radioactivity can be seen in the control (C) nontargeted neuroblastoma, IGR-N-835. The tumor was manually delineated using a cobalt pencil (large arrow). "H" indicates the head of the animals and "Sd" the internal standard.

original sites of uptake and because the lateral resolution of such autoradiograms exceeds 500 nm.

SIMS Mapping and Counting of MBBG

SIMS always exhibited a specific signal for stable bromine, regardless of the tissue section analyzed, the sample processing method applied and the amount of MBBG injected. With chemical sample processing, the tissue structure was well preserved and nucleoli could be visualized on the ^{26}CN ion images. With 102- μm wide image fields (Fig. 4), many cells appeared positive for MBBG, especially in the vicinity of the lumen of vessels. With cryoprepared fragments and 60- μm wide fields, MBBG and MIBG were simultaneously detected. Both drugs were mainly accumulated in the cytosol of the tumor cells (Fig. 5). Although both drugs had rather homogeneous distribution patterns in most of the analyzed areas, which correlates with the tumor model, we found that MBBG was also able to accumulate intensely in several foci of the tumor (Fig. 6). Finally, similar images of MBBG distribution were obtained using either ^{79}Br or ^{81}Br for drug detection, thus providing a powerful internal control for image specificity (Fig. 7).

Local quantification of MBBG uptake, corresponding to 2440 measurements, is given in Table 2. It appears that the higher the injected dose the higher the mean local drug concentration; wide discrepancies, however, were found among the 8- μm wide counting areas, with variations in the range of concentration as large as 80 μg of drug per mg of tissue. In addition, many local concentration values were 10–80 times above the values expected according to radioactive uptake experiments. Finally, we found that the intensities of the secondary standardized bromine ion beams, obtained on 102- μm sputtered areas, were highly correlated ($r = 0.997$, $p < 10^{-4}$), which is in agreement with their similarity in abundance.

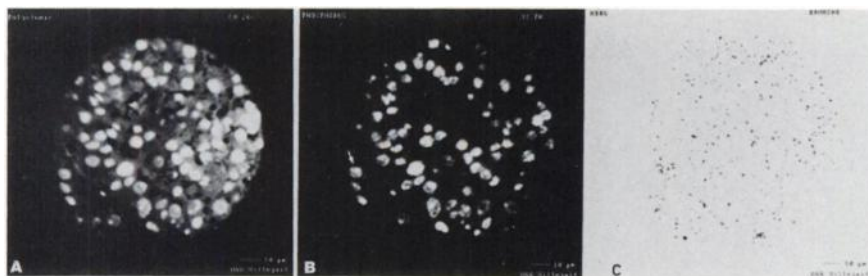


FIGURE 4. SIMS images of [⁸¹Br]MBBG within the PC12 xenograft after in vivo administration of 200 μg of the drug and chemical sample processing. (A) SIMS image of the tissue structure is delineated through polyatomic ²⁶CN (cytosol and nuclei). (B) Phosphorus (³¹Ph) SIMS image mapping of the nuclei and (C) SIMS mapping of MBBG through ⁸¹Br detection, displayed in inverse video scale. On the phosphorus image (B), nucleoli are visible (small arrows), but better mapping of the whole tissue structure is obtained with ²⁶CN detection. MBBG intratumor distribution appears rather homogeneous due to the chemical sample processing. Note the marked staining of the cells close to the vessels. Image field: 102 μm, bar: 10 μm.

DISCUSSION

The use of transplantable tumor models endowed with the same specific uptake and storage systems as those encountered in chromaffin tissue and related tumors is a prerequisite to reliably mimic tracer uptake by tumor cells in humans. Indeed, most human tumors had ischemic and necrotic regions with potentially decreased radiosensitivity and in which radionuclide accessibility may be critical (2). The PC12 pheochromocytoma tumor model was considered appropriate for in vivo pharmacological studies because its avidity for MIBG was retained at a high level after xenografting.

Images of both MBBG and MIBG intratumor uptake were constantly obtained with the IMS-3F. Although both drugs were taken up within a few hours after injection, SIMS experiments were performed 24 hr later. Indeed, the amount of drug taken up at 24 hr is a more reliable gauge of cumulated activity, and thus at mean absorbed dose levels. The 200- and 400-μg of stable drugs injected yielded blood concentration levels bordering on 1 μM 24 hr postinjection (0.34% ID/g of blood and for MBBG), a value known to authorize significant passive diffusion in tumor cells. Because a concentration gradient exists between the blood and tumor cells, however, blood concentrations overestimate the amounts of drug which effectively reach the tumor. In addition, the PC12 xenografts had very high specific uptake values compared to those of nontargeted tissues. Overall, intratumor MBBG or MIBG levels, which may result from passive diffusion, such as in the nontarget

IGR-N-835 neuroblastoma, and even after a 400-μg injected dose, correspond to local concentration values which are below the detection threshold of the IMS-3F for halogens (14,19).

MBBG and MIBG intratumor distribution patterns were crudely homogeneous, but MBBG could also be mapped as rather intense foci of accumulation, especially when the cryopreservation procedure was used. Indeed, the redistribution of stored drugs cannot be ruled out during chemical sample processing due to passive drug diffusion in solvents. This is why cryotechniques ought to be used to ensure signal specificity and to preserve the actual drug concentration levels required for SIMS quantification (20). The focal pattern of accumulation with MBBG remains unexplained. This molecule may gain easier access to tumors because it is much smaller and less lipophilic than MIBG.

Both drugs were shown to accumulate in the cytosol of the tumor cells, but a minute signal was also detected for bromine or iodine when these images were superimposed onto the phosphorus images, which essentially mapped cell nuclei (Fig. 6). Two explanations are plausible here. First, drugs situated in the cytosol but close to the nucleus membrane may be imaged in cell nuclei or at the periphery because the IMS-3F only has a lateral resolution of 500 nm. Second, SIMS analysis functions by successive acquisitions directed at selected ions. The typical acquisition times for ²⁶CN⁻ and ³¹P⁻ are 15–30 sec, whereas duration values bordering 90 sec are often needed to analyze bro-

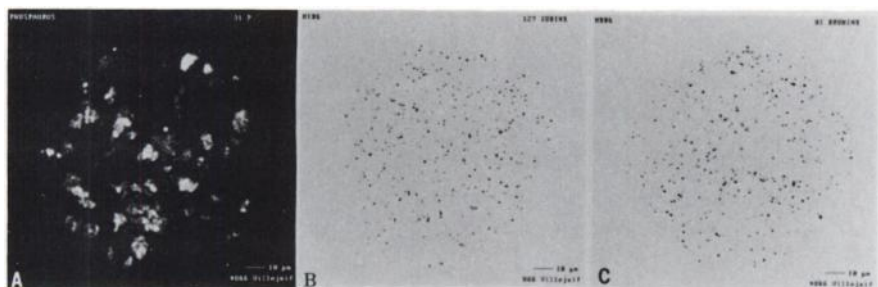


FIGURE 5. SIMS images of MBBG and MIBG within the PC12 xenograft after in vivo administration of 400 μg of the drugs and sample processing with the cryotechniques. The phosphorus image (A) maps tumor cell nuclei which appear very irregular. Both stable MIBG (B) and MBBG (C) exhibited homogeneous intratumor distribution that correlates with the tumor model. There are, however, distributions that cannot be superimposed. Image field: 60 μm.

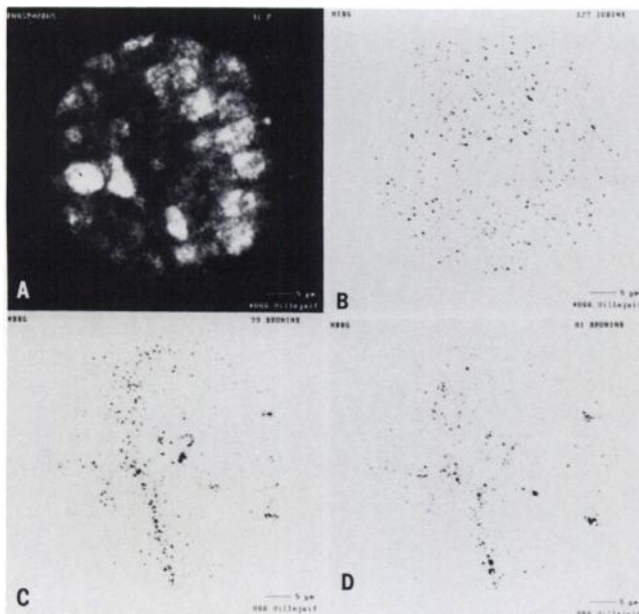


FIGURE 6. SIMS images of MBBG and MIBG within the PC12 xenograft after in vivo administration of 400 μg of the drugs and sample processing with cryotechniques. The phosphorus image indicates the tissue structure (A). Here, ^{127}I MIBG is rather homogeneously distributed (B) compared to MBBG, which shows foci of accumulation (C and D). Because bromine has two stable isotopes of similar abundance, it is possible to map MBBG through the detection of ^{79}Br MBBG (C) or ^{81}Br MBBG (D). Both images are very similar and thus provide a powerful internal control for specificity detection. The minute differences observed between (C) and (D) are due to the fact that the two SIMS images are actually separated by approximately 50 nm. Image field: 60 μm .

mine or iodine, so much so that a depth of 100–300 nm may separate the first and last sputtered plans which ultimately produce the final ionic image. This phenomenon causes a further reduction of ten or so nanometers in the lateral resolution of the composite image resulting from the superimposition of the computerized elementary ionic images. Most of these problems will be solved with the new generation of SIMS microscopes which offer parallel detection and a lateral resolution attaining 50 nm (21). These microscopes are ten times more sensitive than the IMS-3F whose halogen detection threshold is 0.5 $\mu\text{g/g}$ for biological materials with a spatial resolution of below 1 μm .

Local quantification, standardized with the ^{12}C secondary current, was first achieved on 8- μm wide areas, a size well adapted for most problems of cell biology. Counting on cell-scaled areas not only led to a wide range of local concentration values, but also to overestimations compared to the expected mean values derived from radioactive counting. A similar phenomenon, albeit limited, has been reported in the counting of freshly organified iodine in thyroid follicles (22). This may be because very different molar drug doses are considered, ranging from micrograms in SIMS analyses to picograms in radioactive experiments. This also indicates that the sputtered volumes (mg tissue) involved in SIMS analysis are very small and may or may not correspond to sites of drug accumulation. To obtain data more adaptable for multicellular dosimetry, SIMS analysis was also performed on 102- μm wide fields. Unfortunately, we were unable to obtain standardized MBBG local concentration values in our analysis of these larger fields because the standard calibration curves had only been derived for small volumes of tissue-equivalent resin

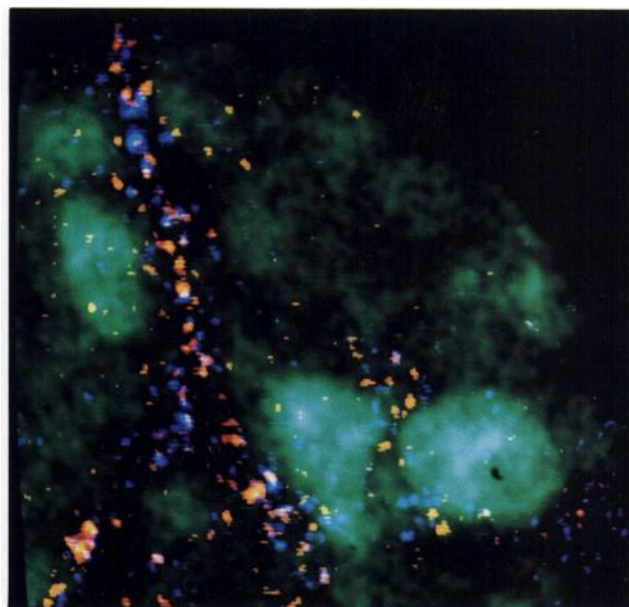
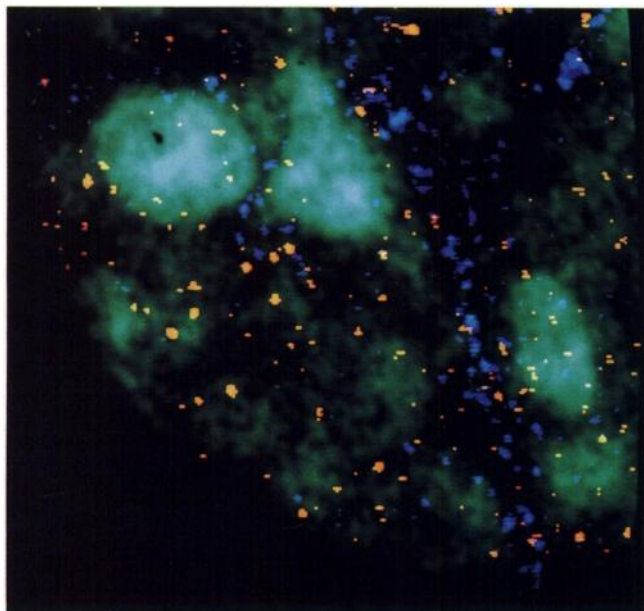


FIGURE 7. SIMS images of superimposed elemental ion images in pseudocolors corresponding to a zoomed detail view of the lower corner in Figure 5. The nuclei are displayed in green (^{31}P). (Left) MIBG is imaged in red-to-yellow and MBBG in blue. Note that most of the signal is evidenced in the perinuclear areas, but that MIBG and MBBG distributions are not superimposable. (Right) MBBG mapping obtained through the detection of ^{79}Br (red) or of ^{81}Br (blue).

TABLE 2
SIMS Quantification of Local Concentration of MBBG within PC-12 Tumors

Injected dose (μg)	N	Normalized ^{79}Br counts ($^{79}\text{Br}/^{12}\text{C}$) $\times 10^{+3}$	Drug concentration mean \pm s.d.	(μg drug/mg tissue) range
200	730	3.38 \pm 4.3	7.88 \pm 10.1	(0–75.6)
200	470	4.23 \pm 6.0	9.92 \pm 14.3	(0.3–80.2)
200	800	2.64 \pm 1.76	6.02 \pm 3.84	(0–17.84)
400	230	7.66 \pm 6.71	18.4 \pm 16.1	(2.76–65.3)

SIMS quantification of the drug is derived from measurements of secondary ^{79}Br ion beam intensity. This current is standardized by the corresponding ^{12}C secondary ion beam intensity and the drug concentration is then derived from calibration curves determined for the same normalized ionic ratio ($^{79}\text{Br}/^{12}\text{C}$) counted in tissue-equivalent resin. N is the number of measurements for each count lasting 1 sec. Two dose levels of injected MBBG are presented. All measurements are made on cryoprepared fragments. The normalized ionic ratio value of <0.002 corresponds to an undetectable local concentration.

and were only available for bromine-to-carbon ratios over 0.002. A comparison of the local concentrations of both drugs was nonetheless obtained by measuring the normalized secondary bromine and iodine ion beams ($^{79}\text{Br}/^{12}\text{C}$ versus $^{127}\text{I}/^{12}\text{C}$) corresponding to the sputtering of these 102- μm wide areas. Both emissions were moderately correlated ($r = 0.3$ to 0.5 , $n = 1200$ measurements, $p < 10^3$) for all analyzed areas, suggesting that uptake mechanisms at the cellular level, though highly specific, only partially account for global uptake in xenografts.

SIMS promises to be a powerful tool in the field of tracer development. Compared to quantitative autoradiography, which has the advantage of being widely available, only SIMS is able to map and quantify multiple stable drugs simultaneously. In addition, not all radioactive isotopes are able to provide autoradiograms with acceptable sensitivity or lateral resolution, and, even when they are suitable, their use in humans is problematic for obvious ethical and legal reasons. Finally, because of filtering by mass spectrometry, all SIMS images have the same lateral resolution, irrespective of the physical decay properties of the analyzed ions under study. Depth-counting profiles have already been obtained with SIMS in biological specimens, and three-dimensional imaging is under development. This technique is complementary to fluorescent confocal microscopy, which is particularly interesting since it provides three-dimensional images of the distribution of monoclonal antibodies directed at tumor antigens or receptors.

Some of the partial responses with MIBG therapy are likely to reflect dramatic heterogeneity in dose distribution, as previously demonstrated in experimental neuroblastoma (19), because 90% of the dose is delivered within 815 μm of a point source with ^{131}I . Among the alternative halogens that can be attached to benzylguanidines, ^{76}Br has favorable physical characteristics for both imaging and therapy. Moreover, PET emission may permit accurate external quantification of tumor compared to that expected with SPECT or planar images, with the added advantage of being able to provide better spatial resolution (10).

MBBG has interesting properties for therapy since it decays through two highly energetic beta emissions (3.1

and 3.6 MeV), which account for particles with path lengths ten times the values reached with ^{131}I . This property is particularly needed when the objective of internal radiotherapy is to kill tumor nodules above 5 mm, and even more so to obtain tumor shrinkage by administering the tracer de novo, i.e., as first-line therapy (23). Indeed, in internal radiotherapy, the probability of tumor cure is maximal for a critical tumor size, which depends on the mean range of the particles emitted. This size has been calculated to be of approximately 2 mm for experimental spherical tumor models when ^{131}I is used (24). The physical half-life (16.2 hr) of ^{76}Br is acceptable for therapy and sufficiently long to permit delivery from distant cyclotron facilities. Finally, no unwanted thyroid irradiation will occur with this drug because bromine, unlike iodine, is not trapped by this gland.

CONCLUSION

It is noteworthy that the range of ^{76}Br in tissue could be of interest to guide the surgeon during surgery and permit the selective detection of labeled tissues from the surface to a few millimeters in depth because intraoperative beta probes are insensitive to gamma radiation (25).

We now know that MBBG will reduce the heterogeneity of dose distribution. The next step is to evaluate whether human tumors will take up MBBG and determine bone marrow toxicity, the dose-limiting factor with MIBG.

ACKNOWLEDGMENT

The authors thank Ms. L. Saint-Ange for editing the manuscript.

REFERENCES

- Shapiro B. Summary, conclusions, and future directions of [^{131}I]metaiodobenzylguanidine therapy in the treatment of neural crest tumors. *J Nucl Biol Med* 1991;35:357–363.
- Shapiro B, Sisson JC, Wieland DM, et al. Radiopharmaceutical therapy of malignant pheochromocytoma with [^{131}I]metaiodobenzylguanidine: results from ten years of experience. *J Nucl Biol Med* 1991;35:269–276.
- Fielding SL, Flower MA, Ackery DM, Kemshead J, Lashford LS, Lewis J. The treatment of resistant neuroblastoma with ^{131}I -MIBG: alternative methods of dose prescription. *Radiotherapy Oncol* 1992;25:73–76.
- Smets LA, Rutgers M. Model studies on metaiodobenzylguanidine (MIBG)

- uptake and storage: relevance for ^{131}I -MIBG therapy of neuroblastoma. *J Nucl Biol Med* 1991;35:191-194.
5. Krempf M, Lumbroso J, Mornex R, et al. Treatment of malignant pheochromocytoma with [^{131}I]metaiodobenzylguanidine: a French multicenter study. *J Nucl Biol Med* 1991;35:284-287.
 6. Shulkin BM, Sisson JC, Koral KF, Shapiro B, Wang X, Johnson J. Conjugate-view gamma camera method for estimating tumor uptake of iodine-131-meta-iodobenzylguanidine. *J Nucl Med* 1988;29:542-548.
 7. Ott RJ, Tait D, Flower MA, Babich JW, Lambrecht RM. Treatment planning for ^{131}I -MIBG radiotherapy of neural crest tumours using ^{124}I -MIBG positron emission tomography. *Br J Radiol* 1992;65:787-791.
 8. Montaldo PG, Carbone R, Ponzoni M, Cornaglia-Ferraris P. Gamma-interferon increases metaiodobenzylguanidine incorporation and retention in human neuroblastoma cells. *Cancer Res* 1992;52:4960-4964.
 9. Iavarone A, Lasorella A, Servidei T, Riccardi R, Mastrangelo R. Uptake and storage of m-iodobenzylguanidine are frequent neuronal functions of human neuroblastoma cell lines. *Cancer Res* 1993;53:304-309.
 10. Valette H, Loc'h C, Mardon K, et al. Bromine-76-metabromobenzylguanidine: a PET radiotracer for mapping sympathetic nerves of the heart. *J Nucl Med* 1993;34:1739-1744.
 11. Galle P. Tissue localization of stable and radioactive nuclides by secondary ion microscopy. *J Nucl Med* 1982;23:52-57.
 12. Smets LA, Janssen M, Rutgers M, Ritzen K, Buitenhuis C. Pharmacokinetics and intracellular distribution of the tumor-targeted radiopharmaceutical m-iodobenzyl-guanidine in SK-N-SH neuroblastoma and PC12 pheochromocytoma cells. *Int J Cancer* 1991;48:609-615.
 13. Loc'h Ch, Mardon K, Valette H, Brutesco C, et al. Preparation and pharmacological preparation of [^{76}Br]-meta-bromobenzylguanidine ([^{76}Br]-MBBG). *Nucl Med Biol* 1994;21:49-55.
 14. Bettan-Renaud L, Bayle Ch, Teyssier JR, Benard J. Stability of phenotypic and genotypic traits during the establishment of a human neuroblastoma cell line, IGR-N-835. *Int J Cancer* 1989;44:460-466.
 15. Fragu Ph, Briançon C, Fourré C, Clerc J, Jeusset J, Halpern S. How can SIMS microscopy be used in biomedicine? *Microbeam Analysis* 1993;2:199-207.
 16. Olivo JC, Khan E, Halpern S, Briançon C, Fragu Ph, Di Paola R. Micro-computer system for ion microscopy digital imaging and processing. *J Microscopy* 1989;56:105-114.
 17. Fourré C, Halpern S, Jeusset J, Clerc J, Fragu Ph. Significance of secondary ion mass spectrometry microscopy for technetium-99m mapping in leukocytes. *J Nucl Med* 1992;33:2162-2166.
 18. Jeusset J, Halpern S, Briançon C, Garcia F, Fragu Ph. Halogen standardization by SIMS microscopy for applications in biological samples [Abstract] *Biol Cell* 1992;75:8a.
 19. Clerc J, Halpern S, Fourré C, Omri B, Jeusset J, Fragu P. SIMS microscopy imaging of the intratumor biodistribution of metaiodobenzylguanidine in the human SK-N-SH neuroblastoma cell line xenografted into nude mice. *J Nucl Med* 1993;34:1565-1570.
 20. Hippe-Sanwald S. Impact of freeze substitution on biological electron microscopy. *Microsc Res Tech* 1993;24:400-422.
 21. Slodzian G, Daigne B, Girard F, Boust F, Hillion F. Scanning secondary ion analytical microscopy with parallel detection. *Biol Cell* 1992;74:43-50.
 22. Briançon C, Halpern S, Jeusset J, Fragu Ph. Effects of various iodine intake on iodine thyroid autoregulation. Study with analytical ion microscopy and ^{129}I . *J Biol Trace Element Res* 1992;32:267-273.
 23. Hoefnagel CA, De Kraker J, Voûte PA, Valdé Olmos RA. Preoperative [^{131}I]metaiodobenzylguanidine therapy of neuroblastoma at diagnosis ("MIBG de novo"). *J Nucl Biol Med* 1991;35:248-251.
 24. Amin AE, Wheldon TE, O'Donoghue JA, Barret A. Radiobiological modeling of combined targeted ^{131}I therapy and total body irradiation for treatment of disseminated tumors of differing radiosensitivity. *Int J Radiat Oncol Biol Phys* 1993;27:323-330.
 25. Daghighian F, Mazziotta FC, Hoffman EJ, et al. Intraoperative beta probe: a device for detecting tissue labeled with positron or electron emitting isotopes during surgery. *Med Phys* 1994;21:153-157.